Near Surface Geophysics, 2007, 273-282

Non-destructive DC resistivity surveying using flat-base electrodes

E.N. Athanasiou*, P.I. Tsourlos, G.N. Vargemezis, C.B. Papazachos and G.N. Tsokas

Department of Geophysics, School of Geology, Aristotle University of Thessaloniki, 54124 Thessaloniki, Greece

Received March 2006, revision accepted February 2007

ABSTRACT

The application of flat-base electrodes to geoelectrical measurements is examined. This study is motivated by the inability to apply geoelectrical techniques in environments where conventional spike electrodes cannot be inserted into the ground. The performance of flat-base electrodes is examined in various environments, using different measuring modes. It is shown that flat-base electrodes can be satisfactorily used in most cases, producing data that are almost identical to the measurements obtained using standard electrodes. Several case studies in various urban locations in Greece, where flat-base electrodes have been successfully employed, are also presented. The results indicate that flat-base electrodes provide the advantage of a fully non-destructive application and, therefore, the extension of geoelectrical methods to environments that, otherwise, would not have been considered suitable.

INTRODUCTION

Over the last decade, electrical resistivity tomography (ERT) has been extensively used in geophysical investigations (Dahlin 2001). The most common applications of ERT are geological mapping (Caglar and Duvarci 2001), geothermal field exploration (Wright *et al*. 1985), hydrogeological studies (Flathe 1955; Dahlin and Owen 1998), engineering geology studies (Dahlin *et al*. 1994), environmental research (Rogers and Kean 1980; Van *et al*. 1991; Daily *et al*. 2004) and archaeological prospection (Papadopoulos *et al*. 2006).

The rapid development of urban infrastructures and various constructions resulted in the need to use geophysical techniques in urban environments (indoors, paved surfaces, roads, etc.). Among the existing geophysical techniques, the method of ground-penetrating radar (GPR) is highly popular (Daniels 2004), due to its fully non-destructive nature and survey speed. Furthermore, the introduction of the newly developed technique of capacitive resistivity (Kuras 2002) holds the promise of efficient electrical imaging in areas where no (or poor) galvanic contact is possible, but its use is mainly restricted to mapping the shallow subsurface.

Applying standard geoelectrical methods in such environments is understandably not popular since, in these cases, the installation of conventional stainless-steel spike electrodes involves drilling holes through the material, which is very laborious and costly. Moreover, in most cases it is prohibited (e.g. in archaeological sites and engineered structures) since drilling holes will damage the inspected site.

As a result, there is a particular interest in studying techniques which allow resistivity measurements to be made in a non-destructive manner, such as using flat-base electrodes (Moussa *et al*. 1977), and therefore extend the application of ERT to other environments (e.g. urban, indoor, etc.). Carrara *et al*. (2001) demonstrated the application of geoelectrical measurements using copper flat-base electrodes, similar to those presented in this work, on a mosaic floor of a Roman residence. The application of a non-destructive geoelectrical grid to access wall struc-

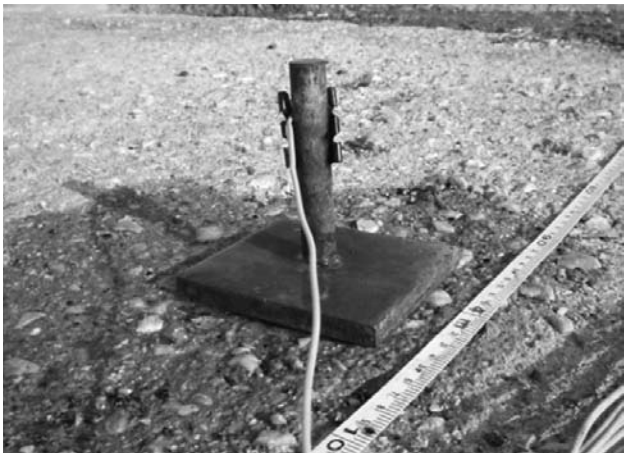

FIGURE 1
Flat-base electrode used in the field applications.

* athanael@geo.auth.gr

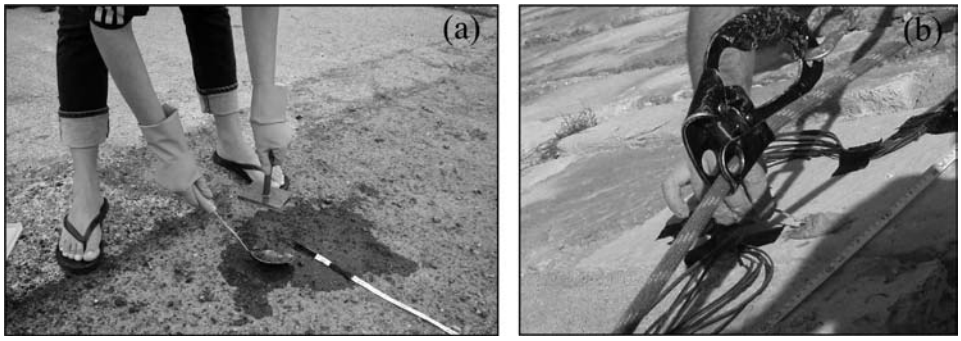

FIGURE 2
(a) Conductive cellulose gel used to ensure that flat-base electrodes are electrically coupled to the surface. (b) Cable contact inserted directly into bentonite plasticine-like electrode.

tures was presented by Cosentino and Martorana (2001), while Karastathis *et al*. (2002) carried out non-destructive ERT measurements on a cement dam in Marathon (Greece).

In this work, we provide some practical guidance and examine several issues related to the application of flat-base electrodes to geoelectrical prospecting. The performance of flat-base electrodes is compared with the performance of conventional spike electrodes. In addition, several field tests are carried out using flat-base electrodes to investigate the effectiveness of the approach. All measured resistivity sections were inverted using a program developed by Tsourlos (1995). The 2D inversion scheme performs an iterative optimization based on a 2.5D finite-element modelling scheme. The algorithm is fully automated and performs smoothness-constrained inversion (Constable *et al*. 1987).

GEOELECTRICAL MEASUREMENTS WITH NON-SPIKE ELECTRODES: PRACTICAL AND THEORETICAL CONSIDERATIONS

The electrodes used in this work consist of a square flat copper base (dimensions: 7 cm × 7 cm, thickness 1 cm), which is placed on the surface of the survey area, and a thin (diameter 1 cm) cylindrical copper segment (length 7 cm) attached to the flat-base part to facilitate cable connections (Fig. 1).

To decrease the contact resistance, a conductive gel was applied between the electrodes and the ground (Fig. 2a). This is extremely important since on relatively rough surfaces the relatively heavy electrode (over 0.5 kg) exerts pressure on the gel which then fills any open voids left between the material and the electrode, thus enabling better contact. Moreover, it was found that spraying the contact area with salt water prior to the application of the gel helped to decrease contact resistance further, particularly during the dry days of the Mediterranean summer (Athanasiou 2004).

TABLE 1
Range of appropriate surface materials for use with flat-base electrodes.

Surface material	Applicability of flat-base electrode
Concrete	✓
Concrete pavement	✓
Pavement stones	✓
Limestone	✓
Marble	✓
Marble stones	✓
Asphalt (tarmac)	×

The gel used in this work consisted of water, salt and low-cost cellulose powder (industrial thickener). Alternatively, conductive gel used in medical applications, or even confectionery gel, was tested successfully although it is generally more costly.
Further, recent tests using bentonite mud (widely used in borehole construction) proved equally effective. In some cases (Tsokas *et al*. 2006), we found that flat-base electrodes could be entirely bypassed by inserting the cable contact directly into bentonite plasticine-like electrodes (Fig. 2b).

It must be noted that successful application of different non-spike electrode types, such as, for example, sponge electrodes saturated with a copper sulphide solution (Karastathis *et al*. 2002) or aluminum foil (Kim 2006, pers. comm.), has been reported. A similar approach is followed by measuring systems using pulled electrode arrays. Systems, such as PACES (Sorensen 1996; Moller and Sorensen 1998) or a similar one developed recently by Iris Instruments (2006), use an array of cylindrical stainless-steel electrodes towed by a vehicle in order to obtain rapid continuous geoelectrical measurements utilizing multichannel resistivity meters. The suggested electrode arrays are heavy enough to establish sufficient galvanic contact with certain types of moist soil.

The above analysis indicates that a variety of materials and techniques exist which can be used to establish electrical contact with earth in a non-destructive manner.

As will be illustrated in the following examples, the electrodes described were used successfully over many commonly encountered materials, such as concrete, concrete pavement, marble plates, etc. (Table 1). Satisfactory contact resistances were routinely achieved (typically 1–3 kΩ), resulting in current intensities that are considered adequate for obtaining accurate and repeatable measurements. The only material over which the technique failed to work was tarmac, a fact that is due to the highly insulating nature of tar.

A problem that is expected to be encountered when non-spike electrodes are used is that the contact resistances are, in general,

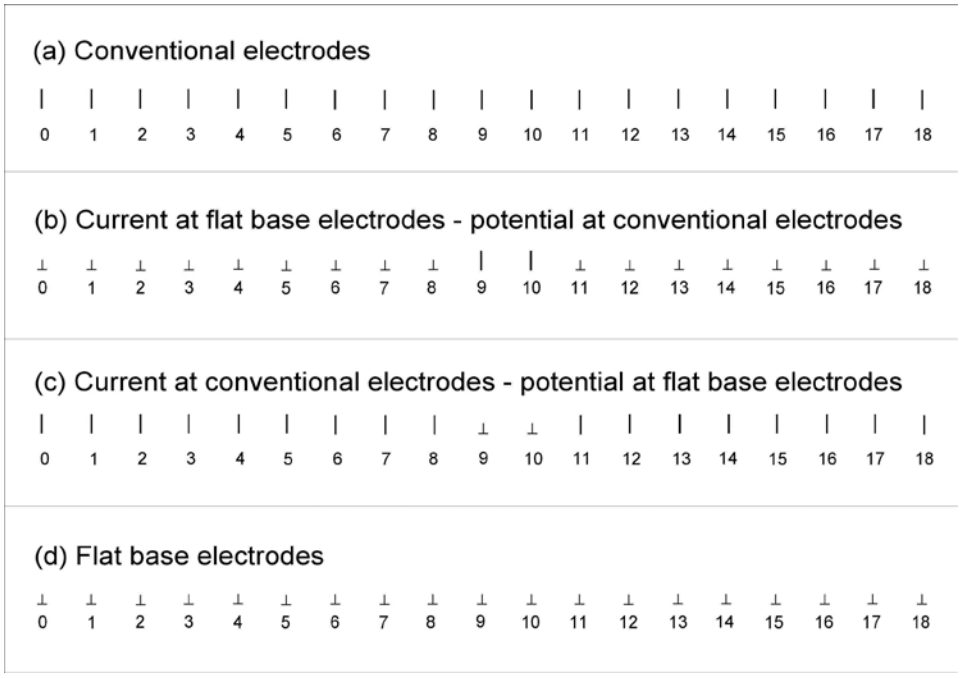

FIGURE 3
Diagram explaining the experimental arrangement of conventional and flat-base electrodes.

expected to be higher than those encountered when using standard spike electrodes. This is not related to the nature or shape of the electrode since the effective contact area between the electrode and the material can be made practically identical in both electrode cases. To give an indication, the flat-base electrodes used in this work have an effective contact area of 7×7 (=49) cm^2, which is almost equivalent to inserting a 1.5 cm diameter standard electrode about 10 cm into the ground.

Contact resistance is mostly related to the moisture content of the contact area. Flat-base electrodes tend to be used on surface material that is generally dryer than the deeper material into which spike electrodes are inserted. Furthermore, the materials usually encountered in surveys of a non-destructive nature are expected to have less moisture than typical soils, since they exhibit either lower porosity or/and they are located indoors. As a result, in this type of survey we tend to encounter higher contact resistances than normally experienced in standard geoelectrical surveys. Consequently, the root-mean-square (RMS) errors produced in the inversions of data sets obtained with flat-base electrodes are expected to be generally higher than normal. Moreover, increased contact resistances suggest that using arrays with a generally good signal/noise ratio in this type of survey is preferable.

A further issue that needs to be addressed is whether flat-base electrodes suffer, due to their shape, from increased modelling errors. Modelling errors encountered in geoelectrical data interpretation are considered negligible when dealing with standard spike electrodes which, even if they are inserted many centimetres into the ground, are treated by forward-modelling routines (e.g. finite-element, finite-difference) as point electrodes. In this framework, the use of flat-base electrodes (of equivalent surface area to spike electrodes) is not expected to produce greater modelling errors. In fact, studies in the field of electrical-impedance tomography using full electrode models on a finite-element mesh suggest that both spike and flat-base electrodes are associated with non-uniform current density distributions (Tungjitkusolmun *et al*. 2000), which are a source of modelling errors.

It is important to note that these modelling errors increase as the inter-electrode spacing decreases, given that the electrode size is fixed, and this holds for both spike and flat-base electrodes. In cases like this, a practical solution, in order to reduce modelling errors, is to use bentonite plasticine-like electrodes, which can be readily shaped to a reduced size.

COMPARISON BETWEEN CONVENTIONAL AND FLAT-BASE ELECTRODE MEASUREMENTS

In order to examine whether flat-base electrodes respond similarly to conventional electrodes, comparative measurements were carried out in various environments, such as soil, concrete, concrete pavement, limestone, etc. Different, commonly used electrode arrays, such as dipole–dipole, Wenner and Wenner–Schlumberger (Loke 2001) with varying spacing, were measured using both electrode types over the same positions (the centres of the flat-base electrodes were placed at exactly the same spots where the conventional electrodes were inserted).

A typical example is described below. Measurements were carried out on soil using 18 conventional and 18 flat-base electrodes in various combinations (Fig. 3a–d). A Wenner–Schlumberger array was used and the spacing *a* between electrodes was 1 metre. The results acquired from flat-base and standard electrodes are illustrated in Fig. 4(a,b,c); they exhibit a good correlation (Fig. 4d) with a relative error of below 1%.

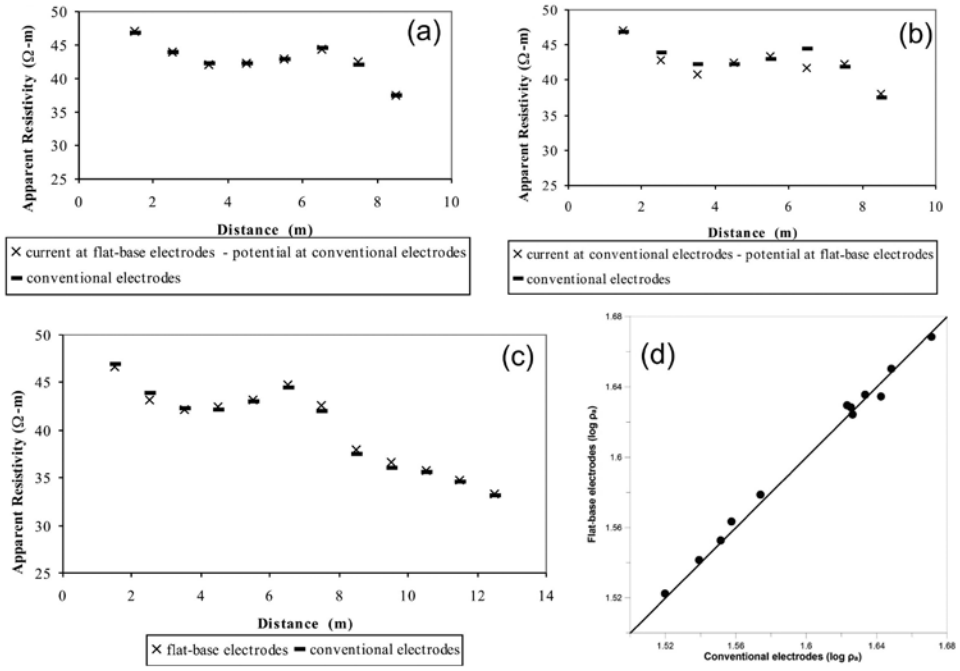

FIGURE 4
(a), (b), (c) Comparison between resistivities acquired from conventional and flat-base electrodes. (d) Correlation between the logarithmic apparent resistivities measured using the two electrode types.

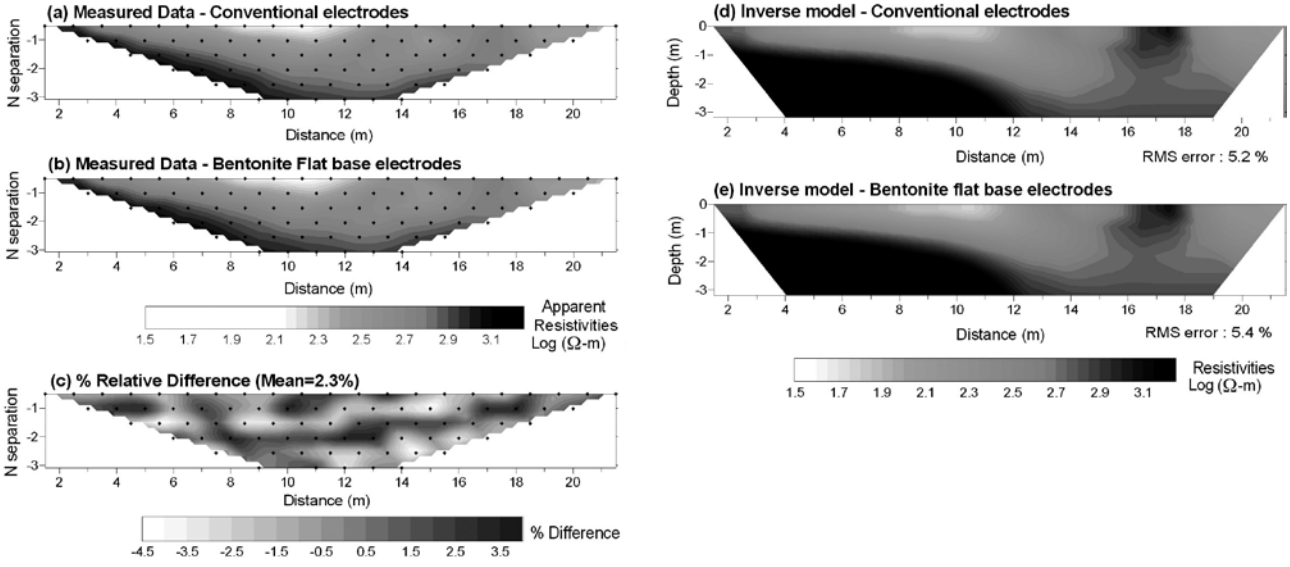

FIGURE 5
Measured apparent-resistivity pseudosections obtained with the Wenner array using (a) conventional electrodes and (b) bentonite flat-base electrodes. (c) Relative differences (%) pseudosection. Inverse models obtained with the Wenner array using (d) conventional electrodes and (e) bentonite flat-base electrodes.

Similar results were obtained in most of our tests.

In order to compare the conventional and flat-base electrode measurements, ERT measurements were carried out using first conventional and then bentonite flat-base electrodes in the same section. The survey was conducted in the Acropolis in Athens, just in front of the Parthenon, and it aimed to detect the limestone bedrock which underlies drift material of varying thickness (0–5 m). The Wenner array was used with 24 conventional and 24 bentonite flat-base electrodes with inter-electrode spacing a of 1 m and maximum n-separation $n_{max}=6a$.

The measured data pseudosections for standard and flat-base electrodes are shown in Fig. 5(a,b), respectively, and the pseudosection of relative differences is depicted in Fig. 5(c). The mean relative difference is 2.3% and no systematic bias is observed.

The geoelectrical inverted models are shown in Fig. (5d,e). It can be seen that the two geoelectrical inverted models acquired using conventional and flat-base electrodes show practically identical information and exhibit similar RMS errors. The limestone bedrock is clearly depicted and a high-resistivity near-surface structure appears at a distance of 17 m along the section, probably corresponding to a wall structure.

A further comparison of the conventional and flat-base electrodes involved measuring ERTs in two parallel sections spaced 0.6 m apart. For the first section, which was situated in a garden, 45 conventional electrodes were used (Fig. 6a). For the second section, which was situated along a pavement, 48 flat-base electrodes were used (Fig. 6b). The garden and the pavement were separated from each other by a metal fence. Although, the two sections were close to each other, the ground structure under the first section was relatively undisturbed while under the second section, especially in the first metres, there had been construction activity (pavement, metal pipes, etc.). The spacing a between electrodes was 5 m with a maximum n-separation n_{max}=7 for electrode spacings of a and 2a. Dipole–dipole, pole–dipole, Wenner–Schlumberger and Wenner arrays were measured. The use of a remote flat-base electrode in the pole–dipole array provided equally good responses when compared with the conventional one.

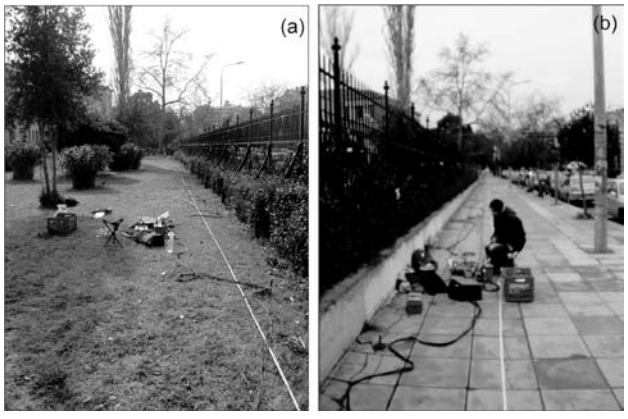

FIGURE 6
Two parallel ERT sections spaced 60 cm apart. (a) The first section, situated in a garden, where conventional electrodes were used; (b) the second section, situated along a pavement, where flat-base electrodes were used. The garden and the pavement were separated from each other by a metal fence.

Two representative geoelectrical inverted models, both obtained by Wenner data sets, are shown in Fig. 7(a, b). The first model (Fig. 7a) was measured using conventional electrodes. The second model (Fig. 7b) was measured using flat-base electrodes. It can be seen that although sharp lateral changes exist in the survey area, the geoelectrical inverted models acquired from the two sections are very similar. Inversion errors were relatively high (10%) but this is attributed to the complex environment where the measurements were carried out. Flat-base inversion exhibits systematically higher RMS errors, of the order of 2–3%. However, it is not clear if this increase is only due to the use of flat-base electrodes or if the complicated shallow structure of the pavement, where the electrodes were placed, contributed to the RMS error increase, given that conventional electrodes exhibited higher RMS errors at the same site. In addition, the contact resistances of the conventional and flat-base electrodes were checked during surveys and were fairly similar.

FIELD APPLICATION EXAMPLES

With the aim of studying the performance of flat-base electrodes further, several field surveys were carried out. All of the examples presented are from sites with well-known structures in order to verify that the results obtained reflect the subterranean reality.

Example 1: Void detection

An air-filled void was exposed at the surface of the concrete pavement of the waterfront at Thessaloniki Bay (Fig. 8). ERT measurements were carried out with the aim of assessing the dimensions of the known void and investigating the existence of other similar voids, which did not appear on the surface (Fig. 9). The surface of the surveyed area was comprised mainly of concrete blocks filled with rubble which had been undermined by the action of seawater, thus creating the above-mentioned voids. Part of the surface had been asphalted in order to cover some of the voids.

Dipole–dipole, pole–dipole, Wenner–Schlumberger and Wenner ERT surveys were undertaken over the study area (Fig. 10a) and a representative geoelectrical inverted model is shown in Fig. 10(b). The measured sections involved 21 flat-

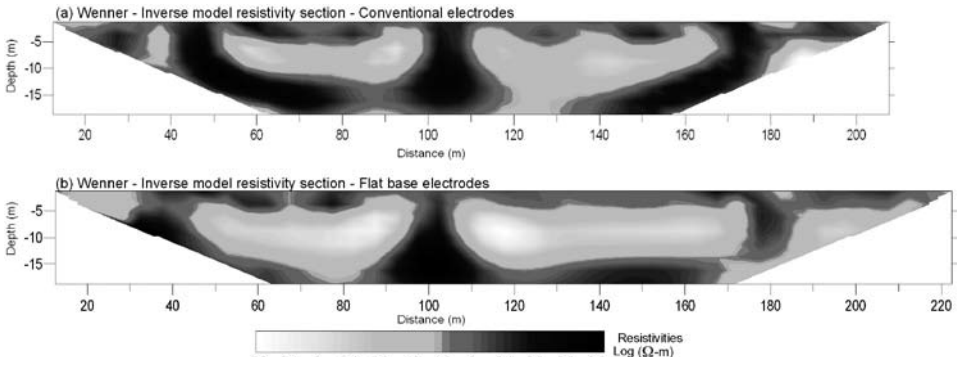

FIGURE 7
Inversion results: Wenner array measured using (a) conventional electrodes and (b) flat-base electrodes.

FIGURE 8
Surface exposure of an air-filled void under the concrete pavement.

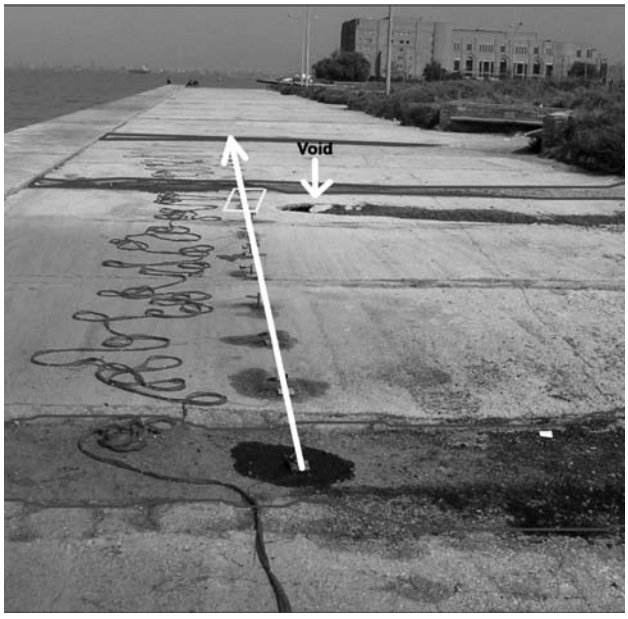

FIGURE 9
ERT using flat-base electrodes across the concrete pavement of the waterfront of Thessaloniki. The exposed void lies at a distance of 8–9 m from the beginning of the tomography array line.

base electrodes with a spacing a of 1 m and maximum n-separation n_{max}=6 for electrode spacings a and 2a.

The inversion results show that the known void is located at a distance of 8–9 m from the beginning of the tomography array line. In addition, a highly resistive body is detected at a distance of 11–12 m, indicating the possible existence of a second void that is not visible at the surface. The sea-level is delineated as a low-resistivity area (resistivity less than 0.2 Ωm), found at a depth of approximately 0.5 m at the beginning of the tomography array line, then gradually descending to increased depths. It must be noted that flat-base electrodes failed to work over tarmac, affecting the measurements that included these particular electrodes.

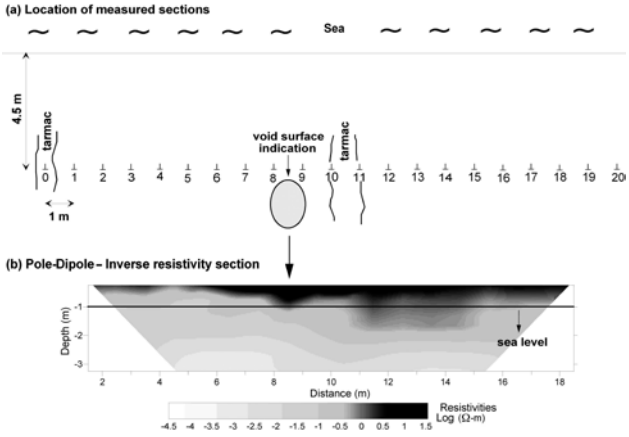

FIGURE 10
(a) Location of the ERT electrodes in relation to the known target. (b) Inverted geoelectrical model obtained by pole–dipole array.

Example 2: Detection of artificial water supplying tunnels (qanat)

In order to locate an ancient *qanat* (a brick-lined tunnel for supplying water) lying under a concrete pavement, ERT measurements were carried out. Dipole–dipole, pole–dipole, Wenner–Schlumberger and Wenner arrays were employed (Fig. 11b) and included 24 flat-base electrodes with a spacing a of 1 m and maximum n-separation n_{max}=7 for electrode spacings a and 2a. The position of this survey line was of special interest because there was a trench at a distance of 2.3 m from the section that provided an impressive 'technical section' (Fig. 11a). The observation of this section showed the exact position of the *qanat* in relation to the measuring section. A moist area was detected on the right side of the *qanat*, and on its left side there was a debris cone, which also preserved high levels of moisture. A manhole was situated at the end of the measuring section, indicating the existence of a sewer under the study area.

Unfortunately, the existence of the large excavated space close to the measuring section affected the measured data and, therefore, no individual geoelectrical configuration could adequately recover the *qanat*. In order to produce a reliable geoelectrical inverted model of the subsurface by taking into account all available information, a combined weighted inversion algorithm of the dipole–dipole and pole–dipole arrays was used (Athanasiou 2004). The combined weighted inverse model resistivity section is shown in Fig. 11(c).

By comparing the exposure of the side of the trench with the geoelectrical combined weighted inverted model, it is clear that there is a very good correlation between the positions of the *qanat* and debris cone and their associated resistivity anomalies. The *qanat* can be identified as an area of high resistivity at a distance of 11–15 m from the beginning of the tomography array line, while the debris cone yields low values of resistivity and is located at a distance of 15–18 m. Low values of resistivity detected on the other side of the *qanat*, at a distance of 7–10 m

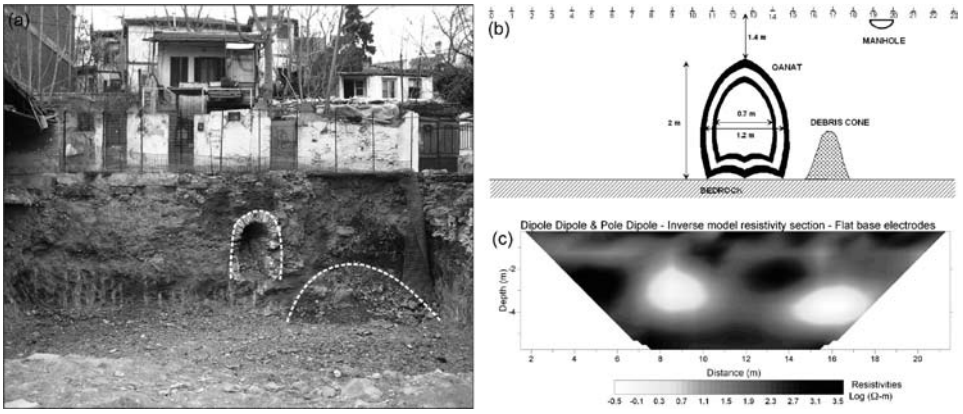

FIGURE 11
(a) Photo of the exposed 'technical section'. (b) Sketch of the 'technical section'. (c) Combined inverted model obtained from dipole–dipole and pole–dipole data sets.

FIGURE 12
Location of the survey area for the bedrock detection test of example 3 (Faculty of Sciences, Aristotle University of Thessaloniki).

from the beginning of the tomography array line, indicate an area of high humidity. The high values of resistivity at shallow depths (~1 m) indicate the existence of other construction activity (pavement, waste pipe).

EXAMPLE 3: BEDROCK MAPPING

The aim of this survey was to locate the bedrock underlying the Faculty of Sciences building of the Aristotle University of Thessaloniki. The bedrock consists mainly of green gneiss that outcrops a few metres northwards from the area of study and underlies recent sediments (clay and sands). The surface formations consist of a man-made ground cover for the first few metres and thereafter alluvial deposits, as well as deposits from the erosion of the bedrock.

Note that the above survey was conducted in an environment complicated by anthropogenic features (pavement, metal pipes, etc.) with expected high levels of measurement noise and modelling errors due to the 3D nature of the inhomogeneities, which are treated with a 2D inversion scheme. Despite the noisy environment, the measurements themselves exhibited a low standard deviation, routinely below 5%.

Dipole–dipole, Wenner–Schlumberger and Wenner arrays were used over the survey area (Fig. 12). The measured section involved 48 electrodes, with spacing a of 3 m and maximum n-separation n_{max}=7 for electrode spacings a and 2a. A representative inverse model resistivity section is depicted in Fig. 13.

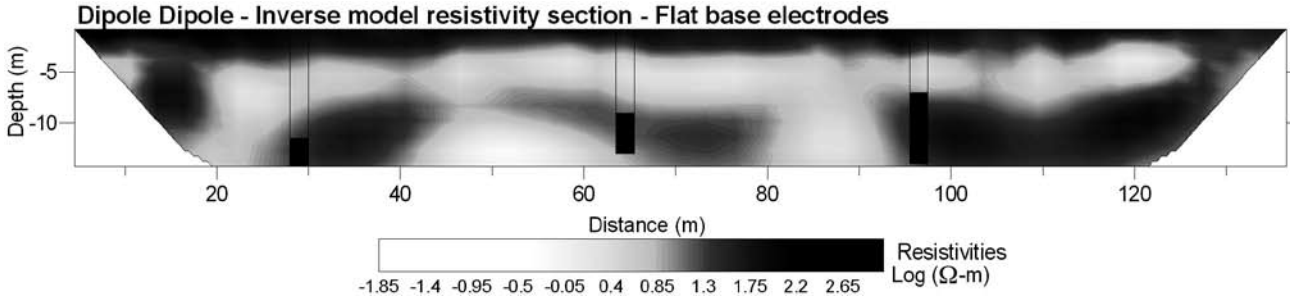

FIGURE 13
Geoelectrical inverted resistivity model obtained by a dipole–dipole array. Black frames represent the location of the boreholes with the bedrock depth indicated by a black bar.

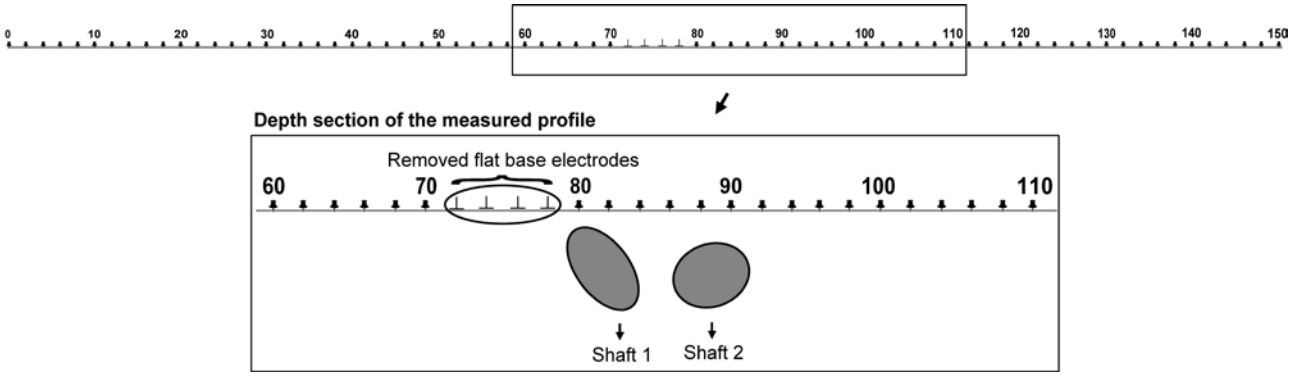

FIGURE 14
Sketch of the measured profile over the known mine shafts. The location of the removed flat-base electrodes is shown.

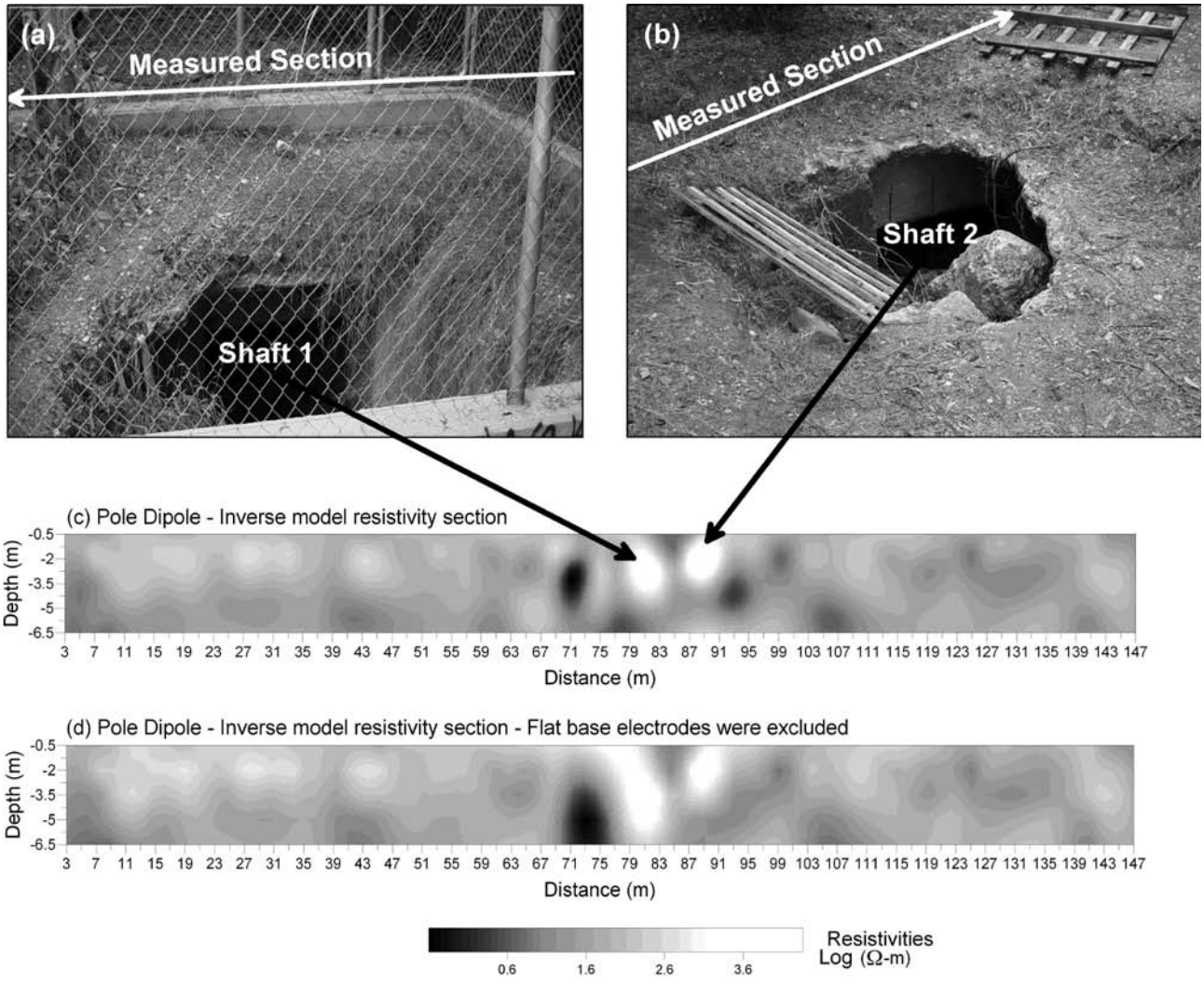

FIGURE 15
(a), (b) Location of the two shafts. (c) Inverted geoelectrical model obtained from a pole–dipole array using mixed conventional and flat-base electrodes. (d) Inverted geoelectrical model obtained from the same pole–dipole array but excluding the identified flat-base electrodes.

Information was also available from three boreholes, which were drilled along the section. Black frames in the inverted section of Fig. 13 are used to depict the position of the boreholes in the inverted model, while the bedrock (gneiss), as recorded by the boreholes, is shown with a filled black bar.

It can be observed that the geoelectrical inversion model is in good agreement with the stratigraphy, as depicted by the boreholes, as far as the depth of the bedrock is concerned, and is identified as an area of high resistivity. The upper surface of the bedrock is interpreted as being at a depth of 11.5 m at the beginning of the section, rising to 9 m within the centre of the section, then finally reaching a depth of 7 m. These depths are confirmed by the borehole information. The high values of resistivity at very shallow depths indicate the existence of rubble originating from anthropogenic activity, as has been observed by previously excavated utility ditches.

EXAMPLE 4: DETECTION OF ABANDONED SHAFTS

The following example deals with an important practical problem commonly encountered in field ERT surveys. In many cases when conducting standard geoelectrical measurements, we are unable to insert spike electrodes either because of man-made structures or due to physical obstacles (namely, outcrops of solid rock, limestone, etc.). Missing electrodes result in incomplete data sets with areas of decreased resolution which can lead to misleading interpretations. This is demonstrated in the example presented, which indicates that in similar cases the use of flat-base electrodes in combination with spike electrodes can eliminate missing data problems.

A site formerly known as the Bodosaki gunpowder factory is situated in the northern part of the park of Aigaleo (Athens). The factory used an expanded network of shafts as vaults for the storage of gunpowder. Today, only the blast furnace at the central part of the study area is preserved. A few surface collapses of the abandoned shafts situated near the blast furnace testify to the existence of this network.

ERT measurements were carried out in order to map the network of the abandoned shafts and to evaluate their dimensions (Tsokas *et al*. 2005). These shafts were built in a geological formation known as the Athenian schist, which was covered by regolith. A number of stone pavements crossed the park and, therefore, the section line. In order to preserve the integrity of the pavements (we were not allowed to drill holes in the pavements), flat-base electrodes were used where appropriate (Fig. 14).

A pole–dipole array was employed using 72 standard and 4 flat-base electrodes with a spacing a of 2 m and a maximum n-separation n_{max}=7. The geoelectrical inversion model is shown in Fig. 15(c). The two known shafts (Fig. 15a, b) are accurately located as areas of high resistivity. The first shaft is located at a distance of 79–84 m from the beginning of the tomography array line and at a depth of 1.25 m below the surface. The second shaft is located at a distance of 86–91 m from the beginning of the tomography array line and at a depth of 0.75 m below the surface.

The inverted resistivity model shown in Fig. 15(d) is obtained from the measured pole–dipole array but with all the flat-base electrodes excluded. It can be seen that the image is quite different from the inversion model obtained with the full array (Fig. 15c). Moreover, the missing information results in a significant modification of the shape and dimensions of the two shafts, especially of the first one, which is closer to the flat-base electrodes.

CONCLUSIONS

The ERT survey tests performed in this study indicate that results obtained with flat-base electrodes are in good agreement with conventional designs. The flat-base electrodes appear to perform well in most environments and with most surface materials except tarmac. Moreover, tests with various electrode arrays indicate that the subsurface geoelectrical structures measured using flat-base electrodes are clearly depicted.

The inversions obtained from the flat-base electrodes had relatively higher RMS errors (of the order of 2–3% more than normally expected), but this can be partly attributed to the complex environments in which our tests were carried out. Using flat-base electrodes can extend the applications of geoelectrical techniques to environments that would not normally be suitable for resistivity tomography. In addition, flat-base electrodes can be also used in combination with standard electrodes in cases where part of the survey area does not allow the use of standard electrodes.

Finally, the use of flat-base electrodes involves dealing with contact resistances that are higher than those normally encountered in geoelectrical surveying. This is expected because flat-base electrodes are placed on the surface, which is usually dry, while conventional electrodes are inserted into materials, which usually retain some level of moisture. This suggests that arrays with a good signal-to-noise ratio (Wenner, Wenner–Schlumberger, pole–dipole) are preferable for this type of survey. In contrast, arrays such as the dipole–dipole may produce low-quality data sets, as is verified by some of our tests.

ACKNOWLEDGEMENT

This work was funded under a doctoral grant scholarship to E.N.A. from the Greek State Scholarships Foundation (IKY).

REFERENCES

Athanasiou E. 2004. *Combined inversion of geoelectrical data by the use of contact electrodes*. MSc thesis, Aristotle University of Thessaloniki.

Caglar I. and Duvarci E. 2001. Geoelectric structure of inland area of Gökova rift, southwest Anatolia and its tectonic implications. *Journal of Geodynamics* **31**, 33–48.

Carrara E., Carrozzo M.T., Fedi M., Florio G., Negri S., Paoletti V., Paolillo G., Quarta T., Rapolla A. and Roberti N. 2001. Resistivity and radar surveys at the archaeological site of Ercolano. *Journal of Environmental and Engineering Geophysics* **6**(3), 123–132.

Constable S., Parker R. and Constable C. 1987. Occam's inversion: A practical algorithm for generating smooth models from electromagnetic sounding data. *Geophysics* **52**, 289–300.

Cosentino P. and Martorana R. 2001. The resistivity grid applied to wall structures: first results. *Proceedings of the 7th Meeting of the Environmental and Engineering Geophysical Society (European Section)*, Birmingham, UK.

Dahlin T. 2001.The development of DC resistivity imaging techniques. *Computers & Geoscience* **27**(9), 1019–1029.

Dahlin T., Johansson S. and Landlin O. 1994. Resistivity surveying for planning of infrastructure. *Proceedings of SAGEEP*, Boston, Massachusetts, USA, pp. 509–528.

Dahlin T. and Owen R. 1998. Geophysical investigations of alluvial aquifers in Zimbabwe. *Proceedings of the IV Meeting of the Environmental and Engineering Geophysical Society (European Section)*, Barcelona, Spain, pp. 151–154.

Daily W., Ramirez A., Binley A. and LaBrecque D. 2004. Electrical resistance tomography. *The Leading Edge* **23**, 438–442.

Daniels D. 2004. *Ground Penetrating Radar*, 2nd edn. The IEE, London, UK.

Flathe H. 1955. Possibilities and limitations in applying geoelectrical methods to hydrogeological problems in the coastal areas of Northwest Germany. *Geophysical Prospecting* **3**, 95–110.

Iris Instruments 2006. *Syscal Pro for Dynamic Acquisition: Land and Marine System for Continuous Resistivity Survey*. www.iris-instrument.com.

Karastathis V.K., Karmis P.N., Drakatos G. and Stavrakakis G. 2002. Geophysical methods contributing to the testing of concrete dams. Application of the Marathon Dam. *Journal of Applied Geophysics* **50**, 247–260.

Kuras O. 2002. *The capacitive resistivity technique for electrical imaging of the shallow subsurface*. PhD thesis, University of Nottingham.

Loke M.H. 2001. A tutorial on 2D and 3D electrical imaging surveys (obtained from www.geoelectrical.com).

Moller I. and Sorensen K.I. 1998. A new approach for fast 2D geoelectrical mapping of near-surface structures. *European Journal of Environmental and Engineering Geophysics* **2**(3), 247–261.

Moussa A.H., Dolphin L.T. and Mokhtar G. 1977. *Applications of modern sensing techniques to Egyptology*. A report of the 1977 field experiments by a joint team. SRI International, Menlo Park, California.

Papadopoulos N.G., Tsourlos P., Tsokas G.N. and Sarris A. 2006. Two-dimensional and three-dimensional resistivity imaging in archaeological site investigation. *Archaeological Prospection* **13**(3), 163–181.

Rogers R.B. and Kean W.F. 1980. Monitoring ground water contamination at a fly ash disposal site using surface resistivity methods. *Ground Water* **18**(5), 472–478.

Sorensen K.I. 1996. Pulled array continuous electrical profiling. *First Break* **14**, 85–90.

Tsokas G., Tsourlos P., Papadopoulos N., Manidaki V., Ioannidou M. and Sarris A. 2006. Non-destructive ERT survey at the south wall of Akropolis of Athens, Greece. Near Surface 2006, Helsinki, Finland, Expanded Abstracts, B040.

Tsokas G., Tsourlos P., Vargemezis G., Sotiropoulos P. and Psarinopoulos N. 2005. ERT and GPR survey for the detection of tunnels in the park of Aegaleo (Athens). Near Surface 2005, Palermo, Italy, Expanded Abstracts, B032.

Tsourlos P. 1995. *Modelling interpretation and inversion of multielectrode resistivity survey data*. PhD thesis, University of York.

Tungjitkusolmun S., Woo E.J., Cao H., Tsai J., Vorperian V.R. and Webster J.G. 2000. Finite element analysis of uniform current density electrodes for radio-frequency cardiac ablation. *IEEE Transactions on Biomedical Engineering* **47**, 32–40.

Van P.V., Park S.K. and Hamilton P. 1991. Monitoring leaks from storage ponds using resistivity methods. *Geophysics* **56**, 1267–1270.

Wright P.M., Ward S.H., Ross H.P. and West R.C. 1985. State-of-the-art geophysical exploration for geothermal resources. *Geohysics* **50**, 2666–2699.